

**Principal Component Abundance Analysis of Microlensed Bulge
Dwarf and Subgiant Stars**B. H. Andrews¹, D. H. Weinberg^{1,2},
J. A. Johnson^{1,2}, T. Bensby³, and S. Feltzing³¹Department of Astronomy, The Ohio State University, 140 West 18th Avenue,
Columbus, OH 43210

email:(andrews, dhw, jaj)@astronomy.ohio-state.edu

²Center for Cosmology and Astro-Particle Physics, The Ohio State University, 191 West
Woodruff Avenue, Columbus, OH 43210³Lund Observatory, Department of Astronomy and Theoretical Physics, Box 43,
SE-22100 Lund, Sweden

e-mail:(tbensby, sofia)@astro.lu.se

Received Month Day, Year

ABSTRACT

Elemental abundance patterns can provide vital clues to the formation and enrichment history of a stellar population. Here we present an investigation of the Galactic bulge, where we apply principal component abundance analysis (PCAA)—a principal component decomposition of relative abundances $[X/Fe]$ —to a sample of 35 microlensed bulge dwarf and subgiant stars, characterizing their distribution in the 12-dimensional space defined by their measured elemental abundances. The first principal component PC1, which suffices to describe the abundance patterns of most stars in the sample, shows a strong contribution from α -elements, reflecting the relative contributions of Type II and Type Ia supernovae. The second principal component PC2 is characterized by a Na–Ni correlation, the likely product of metallicity-dependent Type II supernova yields. The distribution in PC1 is bimodal, showing that the bimodality previously found in the $[Fe/H]$ values of these stars is robustly and independently recovered by looking at only their *relative* abundance patterns. The two metal-rich stars that are α -enhanced have outlier values of PC2 and PC3, respectively, further evidence that they have distinctive enrichment histories. Applying PCAA to a sample of local thin and thick disk dwarfs yields a nearly identical PC1; in PC1, the metal-rich and metal-poor bulge dwarfs track kinematically selected thin and thick disk dwarfs, respectively, suggesting broadly similar α -enrichment histories. However, the disk PC2 is dominated by a Y–Ba correlation, likely indicating a contribution of s-process enrichment from long-lived asymptotic giant branch stars that is absent from the bulge PC2 because of its rapid formation.

Key words: *Galaxy: general — Galaxy: bulge — Galaxy: evolution — Galaxy: formation — Galaxy: stellar content — stars: abundances*

1. Introduction

Elemental abundance trends of Galactic bulge stars are crucial for understanding bulge formation. Galactic chemical evolution is best traced by dwarf stars because their spectra are straightforward to analyze (Edvardsson *et al.* 1993). However, observations of bulge dwarfs are challenging due to their faintness ($V=19-20$; Feltzing and Gilmore 2000), impeding spectroscopic observation under normal circumstances. Consequently, many studies have focused on giant stars, despite the difficulty in analyzing their spectra. This difficulty has led to shifts in the mean $[\text{Fe}/\text{H}]$ and the $[\text{Fe}/\text{H}]$ distribution function of the bulge as the analysis techniques are refined (*e.g.*, Rich 1988, McWilliam and Rich 1994, Fulbright *et al.* 2007, Zoccali *et al.* 2008, Hill *et al.* 2011). Fortunately, gravitational microlensing offers a unique opportunity to observe bulge dwarfs. When a bulge dwarf is lensed by a foreground object, its brightness can increase by >5 magnitudes, enabling spectroscopic observations of sufficiently high resolution and signal-to-noise (S/N) for an abundance analysis (*e.g.*, Minniti *et al.* 1998, Johnson *et al.* 2007, Bensby *et al.* 2011 and references therein).

The abundances of different elements are correlated, reflecting their origin in a common nucleosynthetic process, such as Type II or Type Ia supernovae (SNe). However, these correlations are not perfect because the same element can be made in multiple nucleosynthetic processes, whose relative contributions to a star are best distinguished if abundances are measured for many elements. Here we analyze a sample of 35 bulge dwarfs¹, all of which have at least seven measured elemental abundances and the majority (24/35) of which have 11 or 12 measured elemental abundances, with median errors $\sigma < 0.25$ dex. Bensby *et al.* (2011) find that the bulge dwarf $[\text{Fe}/\text{H}]$ distribution function is bimodal, peaked at $[\text{Fe}/\text{H}] \approx -0.6$ and $+0.3$. They further show that the α -element abundances in the bulge dwarfs vary systematically with $[\text{Fe}/\text{H}]$, following the trends found for thin and thick disk dwarfs (Bensby *et al.* 2003, 2005, Reddy *et al.* 2003, 2006). Here we revisit this data set with a different analysis technique based on principal component decomposition of the elemental abundance patterns, showing that the bimodality seen in $[\text{Fe}/\text{H}]$ also appears in the *relative* elemental abundance patterns.

Principal component analysis (PCA) is a natural tool for characterizing correlations in a high-dimensional space, reducing the overall dimensionality of the data set while allowing the data themselves to reveal the strongest patterns of correlations. While PCA has a long history in astronomy, its application to elemental abundance analysis is relatively new. The only such application we know of is the study of Ting *et al.* (2012), who used this technique to investigate the distributions in elemental abundance space (hereafter, C -space; Freeman and Bland-Hawthorn 2002) defined by various samples of stars from the disk, halo, clusters, and satellite

¹Although our sample includes some subgiant stars, we will describe it as “bulge dwarfs” for brevity.

galaxies. They found that disk stars occupied about 6 dimensions within the 17-dimensional C -space of the data, but the nucleosynthetic processes likely responsible for the lowest order dimensions changed as a function of $[\text{Fe}/\text{H}]$. Their work demonstrated the potential usefulness of principal component abundance analysis (PCAA) as a way to identify groups of stars with distinct enrichment histories. Here we apply this approach to bulge dwarfs to shed further light on the formation of the Galactic bulge.

2. Method

PCAA defines a new set of orthogonal basis vectors in C -space whose components are chosen to align with the maximum variation within the data not already attributed to lower order components. We use standard PCA (see, *e.g.*, Jolliffe 1986) with the data matrix $\{d_{i,j}\}$ representing the logarithmic abundance² relative to iron of element j for star i : $d_{i,j} = [X_j/\text{Fe}]$ with $X_j = \text{O, Na, Mg, Al, Si, Ca, Ti, Cr, Ni, Zn, Y, and Ba}$ for $j = 1, 2, \dots, 12$. PCA identifies orthogonal eigenvectors $\mathbf{e}_k = \{e_{k,j}\}$ such that the abundance of a given element in a given star can be represented as a sum

$$d_{i,j} = \bar{d}_j + \sum_{k=1}^{N_{\text{PC}}} c_{i,k} e_{k,j}, \quad (1)$$

where $\bar{d}_j = \frac{1}{N_{\text{star}}} \sum_{i=1}^{N_{\text{star}}} d_{i,j}$ is the mean value of $[X_j/\text{Fe}]$ in the full data set and $c_{i,k}$ is the coefficient for the k^{th} PC of star i . The first PC describes the direction in elemental abundance space along which the sample stars exhibit the greatest variation, the second PC describes the direction of the second largest variation, etc. If the number of principal components in the sum is equal to the number of elements measured, then the data can be represented exactly. However, if elemental abundances are correlated so that stars are restricted to a lower dimensional subspace, then the elemental abundances can be represented to good accuracy by a smaller number of PCs.

Our data set comes from the homogeneous elemental abundance and error re-analysis of microlensed bulge dwarfs and subgiants by Bensby *et al.* (in prep.); abundances for 26 of our 35 sample stars have been previously published (Epstein *et al.* 2010, Bensby *et al.* 2010, 2011).

3. Results

The dimensionality of the subspace occupied by stars within the full C -space can be expressed as the number of PCs required to explain the intrinsic variation

²Elemental abundances are defined as $[X/Y] \equiv \log(N_X/N_Y) - \log(N_X/N_Y)_\odot$, with missing data replaced by the average value of that elemental abundance for the other stars.

in the data (*i.e.*, the variation not attributable to observational errors). Ting *et al.* (2012) used Monte Carlo simulations spanning a range of intrinsic dimensionality and variance to show that the true dimensionality was recovered when the cumulative variation of the first k PCs was about 85%. For our sample of microlensed bulge dwarfs, the first 1, 2, and 3 PCs describe 64%, 77%, and 84% of the cumulative variation within the data. Although the threshold for completely describing the data likely depends on many factors including sample size, number of observed abundances, and abundance uncertainties, it is fair to say that the bulge dwarfs occupy approximately three dimensions of the 12-dimensional C -space investigated here.

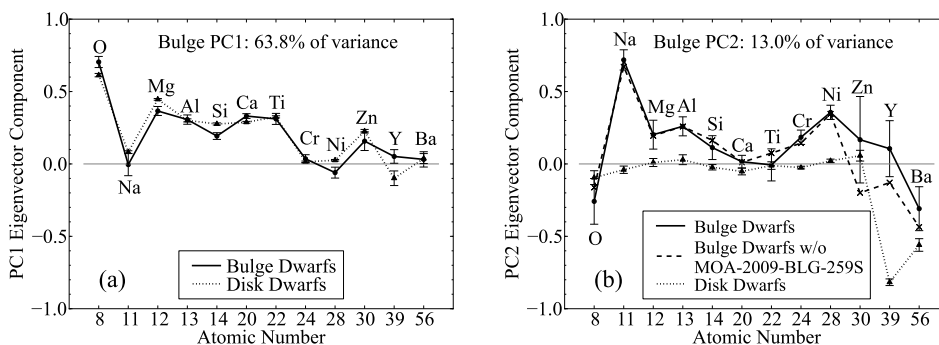


Fig. 1. A graphical representation of the PC1 (panel a) and PC2 (panel b) vectors of the microlensed bulge dwarfs (circles/solid lines) and the disk dwarf sample of Bensby *et al.* (2003, 2005, and in prep.) (triangles/dotted lines). The PC1 and PC2 eigenvector components refer to $e_{1,j}$ and $e_{2,j}$, respectively, from Eq. (1), with uncertainties from bootstrap resampling. We also show PC2 for the bulge dwarfs if MOA-2009-BLG-259S is omitted from the sample (crosses/dashed line in panel b); PC1 remains nearly unchanged, so it is not plotted for clarity. Each symbol represents an abundance (X/Fe) and thus a dimension in the original C -space.

Fig. 1 shows the first two PCs derived from the observed bulge dwarf elemental abundances, with the uncertainties determined from bootstrap resampling (see below). PC1 is dominated by the abundances of oxygen, other α -elements (Mg, Si, Ca, and Ti), and Al, with small uncertainties on the relative contributions of each abundance. SNe II are the primary source of α -elements and Al, but they are also a significant producer of Fe, especially at early times. By contrast, SNe Ia create large amounts of Fe and other Fe-peak elements, leading to sub-solar $[\alpha/\text{Fe}]$ yields; once enough time has elapsed for a substantial number of SNe Ia to occur, they become the dominant source of Fe. The interplay between these two nucleosynthetic sources is thought to underpin the dichotomy in $[\alpha/\text{Fe}]$ observed in Galactic disk stars, with high $[\alpha/\text{Fe}]$ for “thick disk” stars reflecting rapid formation (*e.g.*, Fuhrmann 1998) and roughly solar $[\alpha/\text{Fe}]$ for “thin disk” stars, which have predominantly higher $[\text{Fe}/\text{H}]$ (Gilmore and Wyse 1985). Although PCA is a “blind” statistical technique with no *a priori* theoretical input, in this data set (and others we have explored) the first principal component picks up this expected

distinction between the two dominant supernova enrichment mechanisms.

PC2 is primarily governed by Na with secondary contributions from Ni (correlated with Na) and Ba (anticorrelated with Na). A similar Na–Ni correlation, attributed to metallicity-dependent SN II yields, has been found previously in halo stars (Nissen and Schuster 1997, 2010); however, this study and the companion paper of Bensby *et al.* (in prep.) are the first to identify a Na–Ni correlation amongst bulge stars (see Bensby *et al.* in prep. for more details). Na is primarily produced by hydrostatic carbon burning in the massive stars that explode as SNe II, but proton capture at the same temperatures depletes the pre-explosion Na abundance. As metallicity increases, the neutron excess increases, making Na less susceptible to proton capture and consequently increasing the overall Na yield (Clayton 2003). Similarly, the yield of ^{58}Ni (the most common Ni isotope) from SNe II is sensitive to the neutron excess and the abundance of neutron-rich nuclei, like ^{23}Na , in the progenitor star (Woosley *et al.* 1973). Additional significant ^{58}Ni production occurs in SNe Ia, whose ^{58}Ni yield increases with metallicity (Timmes *et al.* 2003). However, the Na–Ba anticorrelation is not readily explained by a single nucleosynthetic process. One star with distinctive abundances, MOA-2009-BLG-259S (see Fig. 3c), has a large impact on the contributions of Zn, Y, and Ba to PC2 and drives up the uncertainties for these abundances. The crosses/dashed line in Fig. 1b show the effect of omitting this star when defining principal components; PC1 hardly changes, but the contributions of Zn and Y to PC2 switch from being correlated with Na to anticorrelated. The $[\text{Y}/\text{Fe}]$ for MOA-2009-BLG-259S has a large uncertainty, though the elevated $[\text{Zn}/\text{Fe}] = 0.44 \pm 0.17$ appears to be well-established (Fig. 3c). Regardless of MOA-2009-BLG-259S, PC2 is dominated by Na and shows a Na–Ni correlation and a Na–Ba anticorrelation.

For comparison, we have found the principal components of a sample of 702 solar neighborhood thin and thick disk dwarfs from Bensby *et al.* (2003, 2005, and in prep.) with the same elements measured. The disk PC1 and PC2 are shown as triangles/dotted lines in Fig. 1. The clear similarity between the bulge and disk PC1s suggests that the relative enrichment from SNe II vs. SNe Ia is the main driver of diversity among stars in both samples. On the other hand, the disk and bulge PC2s do not resemble each other: in contrast to the bulge PC2 discussed above, the disk PC2 is dominated entirely by correlated Y and Ba, both neutron-capture elements produced mainly by the *s*-process in disk stars (Snedden *et al.* 2008). The short vs. long lifetimes of the nucleosynthetic sources driving the bulge and disk PC2s, respectively, implies that the bulge formed too rapidly (\lesssim Gyr) for asymptotic giant branch stars to dominate PC2. Johnson *et al.* (2012) independently reached a similar conclusion based on the relative abundances of *r*- and *s*-process elements.

Fig. 2 shows the distribution of the 35 bulge dwarfs in (PC1, PC2)-space, with the upper panel showing the histograms of the bulge dwarfs in PC1 and of kine-

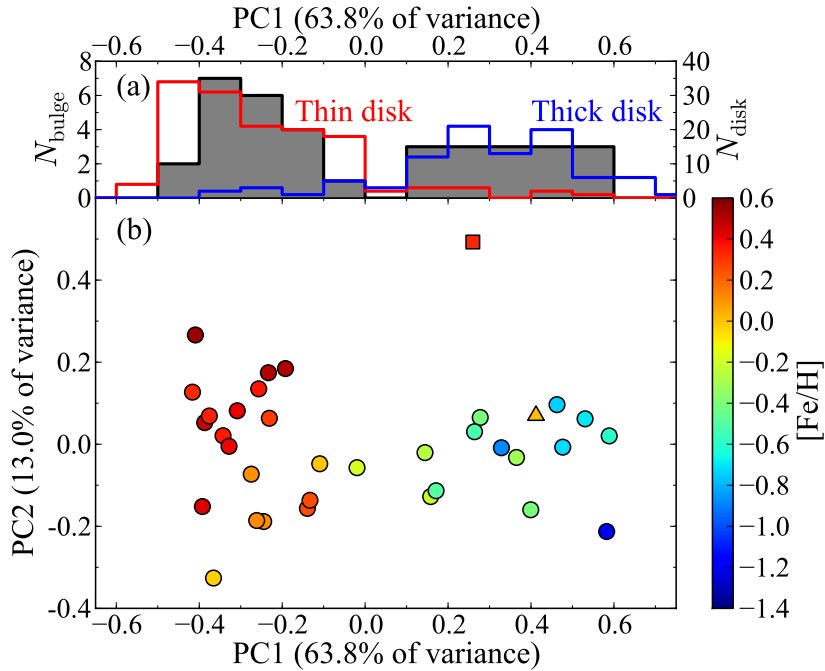


Fig. 2. Panel (a): the histograms of bulge dwarfs (gray) and of kinematically selected thin (red) and thick (blue) disk dwarfs projected onto the bulge PC1 axis defined above. Panel (b): the distribution of bulge dwarfs in (PC1, PC2)-space, color-coded by $[\text{Fe}/\text{H}]$. The square and triangle represent the PC2 outlier (MOA-2009-BLG-259S) and the PC3 outlier (MOA-2010-BLG-523S), respectively. The positions along PC1 and PC2 correspond to $c_{i,1}$ and $c_{i,2}$, respectively, in Eq. (1).

matically selected subsets of thin and thick disk dwarfs³ projected onto the bulge PC1. It is evident from visual inspection that the bulge dwarfs divide into two distinct groups along the PC1 axis, centered at PC1 values of ± 0.3 . (Because the sum in Eq. 1 includes the mean elemental abundances of the sample, a value of $\text{PC1} = -0.3$ corresponds to $\sim [\alpha/\text{Fe}]_{\odot}$.) Thus, this analysis of *relative* elemental abundances, with no direct input from $[\text{Fe}/\text{H}]$, recovers the bimodality that Bensby *et al.* (2011) found in the $[\text{Fe}/\text{H}]$ distribution without reference to relative abundances. Bensby *et al.* (2011) did find elevated $[\alpha/\text{Fe}]$ ratios for the metal-poor bulge dwarfs, and we recover the same correlation in this “reverse” analysis: every star with $\text{PC1} < -0.1$ has $[\text{Fe}/\text{H}] > -0.02$, and all but two of the stars with $\text{PC1} > -0.1$ have $[\text{Fe}/\text{H}] < -0.18$. Of these two stars, one (MOA-2009-BLG-259S; square) is a clear PC2 outlier, while the other (MOA-2010-BLG-523S; triangle) is a moderate PC3 outlier that is undistinguished in (PC1, PC2)-space.

Fig. 2a shows that the metal-rich and metal-poor bulge dwarfs track the thin

³The kinematic designation is based on the Bensby *et al.* (2003) selection criteria; however, we adopt a more stringent cut on the relative thick/thin disk membership probability: stars with $P(\text{thick disk})/P(\text{thin disk}) > 100$ and $P(\text{thick disk})/P(\text{thin disk}) < 0.01$ are designated thick and thin disk stars, respectively.

and thick disk dwarfs, respectively, in PC1. PCAA highlights the scarcity of stars with intermediate $[\alpha/\text{Fe}]$ ($\text{PC1} \sim 0$) in the bulge dwarfs and in the thin and thick disk dwarfs. The fact that the two bulge populations track the two disk populations in $[\text{Fe}/\text{H}]$ and PC1 suggests that the stars had α -enrichment histories that produced the same abundance patterns. This similarity provides tentative evidence that the bulge formed through secular processes, such as disk instabilities, that heated inner thin and thick disk stars to form the bulge (Kormendy and Kennicutt 2004). Alternatively, the bulge and disk could have formed by distinct mechanisms but experienced “convergent” enrichment histories. For example, Bournaud *et al.* (2007) propose that the large cosmological accretion rates of high redshift galaxies enable the rapid (~ 0.5 – 1 Gyr), simultaneous formation of the bulge and inner disk, which could account for the α -enhanced subpopulation of each component.

To test the statistical significance of PC1 and PC2 and the robustness of the bimodality in Fig. 2, we created 100 bootstrap resamplings of the data set, redefining principal components each time. PC1 is always recovered, and the general form of PC2 (high Na value, Na–Ni correlation, and Na–Ba anticorrelation) is recovered in 99/100 resamplings. Thus, PC2 is statistically significant even though the contributions of Zn, Y, and Ba to PC2 fluctuate because of its sensitivity to MOA-2009-BLG-259S. The histogram of PC1 values is always multimodal, showing two distinct groupings (as in Fig. 2a) about 90% of the time; the remaining resamplings show three apparent groupings, but the small sample size makes the distribution of values *within* the $\text{PC1} > 0$ group difficult to characterize reliably. The significance of a formal test for bimodality will depend on the form of the adopted null hypothesis, but the likelihood ratio of a 2-Gaussian fit to the PC1 distribution to a 1-Gaussian fit is $\mathcal{L}(2\text{G})/\mathcal{L}(1\text{G}) = 2 \times 10^5$, a large improvement for the addition of two free parameters.

Fig. 3 shows the decompositions of the elemental abundance patterns of four sample stars into the sum of the sample mean and the first one, two, or three PCs. The best fit coefficients $c_{i,k}$ of Eq. (1) are found for each star by χ^2 -minimization, treating all errors as independent. Panels (a) and (b) show typical examples of metal-poor and metal-rich stars, respectively, each of them fit almost perfectly with a single PC. Panel (c) shows MOA-2009-BLG-259S, which is poorly fit by PC1 alone but well fit when PC2 is also included. Panel (d) shows MOA-2010-BLG-523S, which has one of the largest PC3 coefficients in our sample.

Clearly these PCA fits have low values of $\chi_{\text{red}}^2 = \chi^2/(\text{d.o.f.})$, once a sufficient number of PCs (one, two, or three) is included. The number of degrees of freedom is the number of elemental abundances measured for the star minus the number of PCs in the fit. Panel (e) shows the histogram of χ_{red}^2 values for single-PC and 2-PC decompositions; median values are $\chi_{\text{red}}^2 = 0.31$ and 0.21 , respectively. The low χ_{red}^2 values indicate that the observational errors on the elemental abundances are typically overestimated, at least in the sense that they do not represent the variance in estimated elemental abundance that would arise from observing the same star

many times. We believe that these low χ_{red}^2 values arise because the quoted errors effectively incorporate a component of systematic calibration error in addition to random error. For example, multiple lines of the same element may give discrepant abundance estimates because of uncertainties in the assumed oscillator strengths; the internal dispersion of these estimates is one useful indication of the absolute elemental abundance uncertainty, but the range of elemental abundance measurements from multiple high-S/N spectra will be smaller than this dispersion because the same oscillator strengths are assumed each time. The treatment of random and systematic errors and error correlations is a significant issue for PCAA and other model-fitting approaches, but we defer it to future investigations.

4. Conclusions

Our results confirm and extend the findings of Bensby *et al.* (2011), who identified bimodality in the [Fe/H] distribution of microlensed bulge dwarfs, with metal-poor stars showing enhanced α -element abundances like those of solar neighborhood thick disk stars. Our principal component analysis demonstrates that the bimodality found by Bensby *et al.* (2011) is present even in the *relative* elemental abundances ([X/Fe]) of the bulge dwarfs alone. The first PC is dominated by α -elements, reflecting the dichotomy between SN II and SN Ia enrichment. The second PC captures the Na–Ni correlation caused by the metallicity dependence of SN II yields. Intriguingly, the two metal-rich stars that exhibit α -enhancement (MOA-2009-BLG-259S and MOA-2010-BLG-523S) are also outliers from the main locus of stars in (PC1, PC2, PC3)-space, suggesting that they do indeed have unusual enrichment histories. If we project the thin and thick disk dwarfs onto the bulge dwarf PC1, they occupy the locations of the metal-rich and metal-poor bulge dwarfs, respectively. Analyzing local disk dwarfs, we find that the first principal component is nearly identical to the bulge PC1. However, the disk PC2 is governed by Y and Ba, products of long-lived asymptotic giant branch stars, whereas enrichment from short-lived SNe II drives the bulge PC2. Qualitatively, these results support a scenario in which the bulge grows by secular evolution from the inner disk, which itself has the elemental abundance dichotomy seen in local populations, but there may be other bulge formation models that can produce similar results.

Our results, and those of Ting *et al.* (2012), illustrate the potential of PCAA as a tool for characterizing the distribution of stars in high-dimensional C -space. One application, highlighted here, is to identify subpopulations in a sample, drawing on the information present in all measured elemental abundances simultaneously. With large multi-element samples, this approach could be used to isolate “interloper” stars accreted from a dissolved satellite, and perhaps to identify cohorts of stars associated with common birth clusters (Freeman and Bland-Hawthorn 2002). A second application, illustrated by the examples of MOA-2009-BLG-259S and MOA-2010-BLG-523S, is to identify outlier stars, either through their unusual lo-

cations in PC-space or because they are poorly fit by combinations of PCs that fit most stars well. Such outliers may reveal rare but physically informative enrichment pathways. A third application, highlighted by Ting *et al.* (2012), is to characterize the dimensionality of the stellar distribution in C -space, which is a basic test for models of Galactic assembly and enrichment. We will explore this technique in future work using theoretical models.

By allowing the data themselves to define the directions of strongest variation, PCAA complements the usual approach of testing predictive models that adopt nucleosynthetic yields from theoretical calculations. The PCs clearly do have physical content, but the connection of PCs to enrichment mechanisms is not one-to-one (see Ting *et al.* 2012), and interpreting them will require comparisons to models that vary both enrichment and mixing histories and the nucleosynthetic yields themselves. Our analysis identifies several practical complications of PCAA, including the potential sensitivity to outliers in small samples, the treatment of missing elemental abundance measurements, the impact of heteroscedastic errors and correlated errors, and the mix of random and systematic contributions to the errors quoted in observational analyses. We will investigate these issues in future work. The enormous samples of high-resolution spectra anticipated from the SDSS-III APOGEE survey (Majewski *et al.* in prep., Eisenstein *et al.* 2011), the Gaia-ESO survey (Gilmore *et al.* 2012), and the HERMES survey (Barden *et al.* 2010) will map the elemental abundance distribution over wide swaths of the Galaxy, and PCAA will be a valuable tool for connecting these measurements to a comprehensive theory of the formation of the Milky Way.

Acknowledgements. We acknowledge support of NSF grant AST1009505. T.B. was funded by grant No. 621-2009-3911 from The Swedish Research Council.

REFERENCES

- Barden, S. C., Jones, D. J., Barnes, S. I., *et al.* 2010, *Proc. SPIE*, **7735**, .
- Bensby, T., Feltzing, S., and Lundström, I. 2003, *A&A*, **410**, 527.
- Bensby, T., Feltzing, S., Lundström, I., and Ilyin, I. 2005, *A&A*, **433**, 185.
- Bensby, T., *et al.* 2010, *A&A*, **512**, A41+.
- Bensby, T., *et al.* 2011, *A&A*, **533**, A134.
- Bournaud, F., Elmegreen, B. G., and Elmegreen, D. M. 2007, *ApJ*, **670**, 237.
- Clayton, D. 2003, *Handbook of Isotopes in the Cosmos*, by Donald Clayton, pp. 326. ISBN 0521823811. Cambridge, UK: Cambridge University Press, October 2003., , .
- Edvardsson, B., Andersen, J., Gustafsson, B., Lambert, D. L., Nissen, P. E., and Tomkin, J. 1993, *A&A*, **275**, 101.
- Eisenstein, D. J., *et al.* 2011, *AJ*, **142**, 72.
- Epstein, C. R., Johnson, J. A., Dong, S., Udalski, A., Gould, A., and Becker, G. 2010, *ApJ*, **709**, 447.
- Feltzing, S., and Gilmore, G. 2000, *A&A*, **355**, 949.
- Freeman, K., and Bland-Hawthorn, J. 2002, *ARA&A*, **40**, 487.
- Fuhrmann, K. 1998, *A&A*, **338**, 161.
- Fulbright, J. P., McWilliam, A., and Rich, R. M. 2007, *ApJ*, **661**, 1152.
- Gilmore, G., and Wyse, R. F. G. 1985, *AJ*, **90**, 2015.

- Gilmore, G., *et al.* 2012, *The Messenger*, **147**, 25.
- Hill, V., *et al.* 2011, *A&A*, **534**, A80.
- Johnson, C. I., Rich, R. M., Kobayashi, C., and Fulbright, J. P. 2012, *ApJ*, **749**, 175.
- Johnson, J. A., Gal-Yam, A., Leonard, D. C., Simon, J. D., Udalski, A., and Gould, A. 2007, *ApJ*, **655**, L33.
- Jolliffe, I. T. 1986, *Springer Series in Statistics, Berlin: Springer, 1986*, , .
- Kormendy, J., and Kennicutt, Jr., R. C. 2004, *ARA&A*, **42**, 603.
- McWilliam, A., and Rich, R. M. 1994, *ApJS*, **91**, 749.
- Minniti, D., Vandehei, T., Cook, K. H., Griest, K., and Alcock, C. 1998, *ApJ*, **499**, L175.
- Nissen, P. E., and Schuster, W. J. 1997, *A&A*, **326**, 751.
- Nissen, P. E., and Schuster, W. J. 2010, *A&A*, **511**, L10.
- Reddy, B. E., Lambert, D. L., and Allende Prieto, C. 2006, *MNRAS*, **367**, 1329.
- Reddy, B. E., Tomkin, J., Lambert, D. L., and Allende Prieto, C. 2003, *MNRAS*, **340**, 304.
- Rich, R. M. 1988, *AJ*, **95**, 828.
- Snedden, C., Cowan, J. J., and Gallino, R. 2008, *ARA&A*, **46**, 241.
- Timmes, F. X., Brown, E. F., and Truran, J. W. 2003, *ApJ*, **590**, L83.
- Ting, Y. S., Freeman, K. C., Kobayashi, C., de Silva, G. M., and Bland-Hawthorn, J. 2012, *MNRAS*, **421**, 1231.
- Woolsey, S. E., Arnett, W. D., and Clayton, D. D. 1973, *ApJS*, **26**, 231.
- Zoccali, M., Hill, V., Lecqueur, A., Barbuy, B., Renzini, A., Minniti, D., Gómez, A., and Ortolani, S. 2008, *A&A*, **486**, 177.

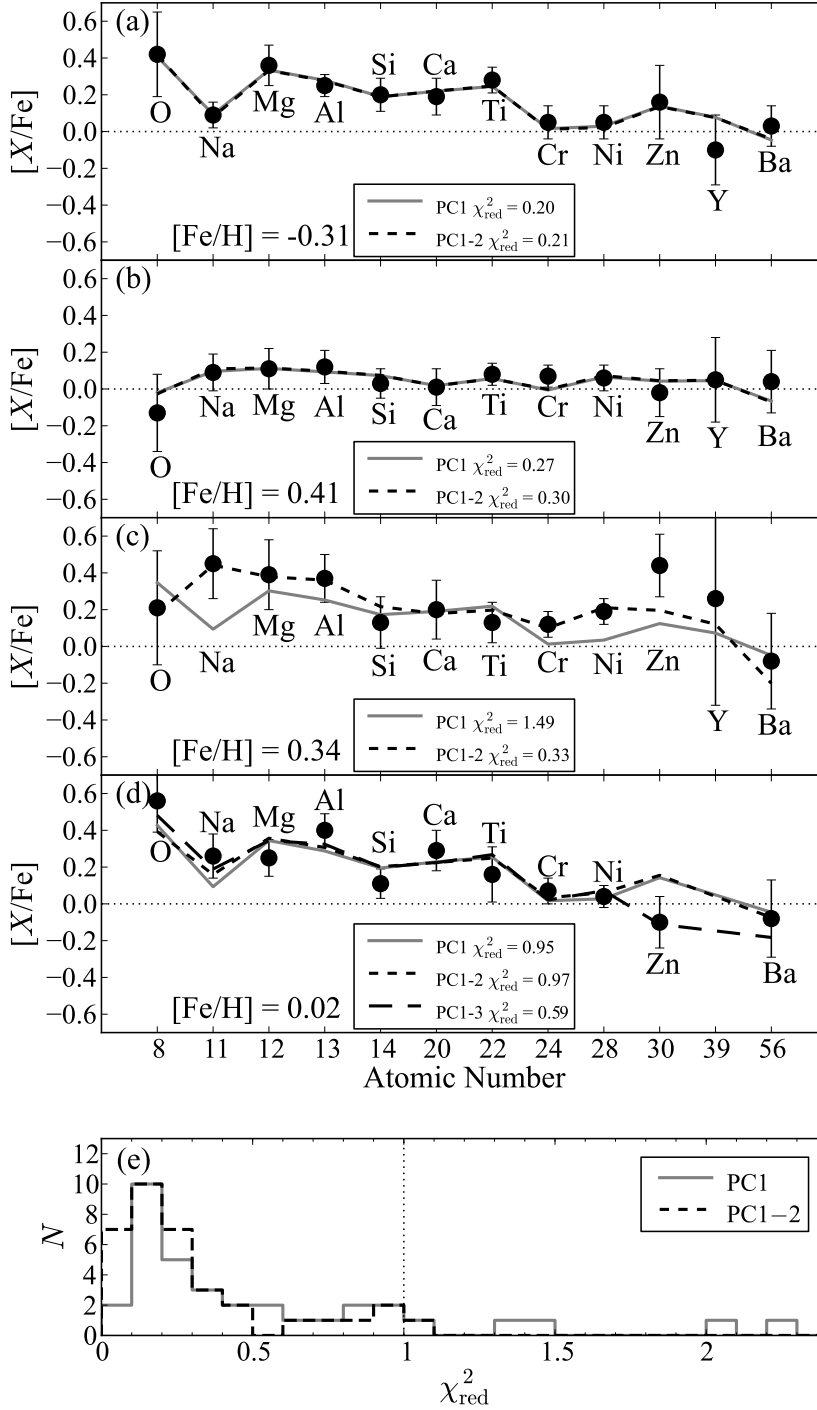


Fig. 3. Panels (a)–(d) show elemental abundances for, respectively, a metal-poor star, a metal-rich star, the PC2 outlier star (MOA-2009-BLG-259S), and the PC3 outlier star (MOA-2010-BLG-523S). Lines indicate the best fit combined abundance pattern using the mean abundance and the first PC (solid gray line), the first two PCs (short dashed line), and the first three PCs (long dashed line in panel d only). Reduced- χ^2 (χ_{red}^2) values for these fits are listed in the legends. Panel (e) shows the distribution of χ_{red}^2 values for the bulge dwarf sample, with the same line types as panels (a)–(c).